Supporting Information for:

A Hexagonal Ni_6 Cluster Protected by 2-Phenylethanethiol for Catalytic Conversion of Toluene to Benzaldehyde

Anthony M.S Pembere[ξ], *Chaonan Cui*[ξ], *Rajini Anumula*[ξ], *Huiming Wu, Pan An, Tongling Liang, Zhixun Luo*[*]

State Key Laboratory for Structural Chemistry of Unstable and Stable Species, Institute of Chemistry, Chinese Academy of Sciences; and University of Chinese Academy of Sciences, Beijing 100090, China.

∗ Correspondence. Email: zxluo@iccas.ac.cn

[ξ] *These authors contributed equally to this paper and share the first authorship.*

This updated version of the Electronic Supplementary Information (published on 20 Feb 2020) replaces the original version first published on-line on 23 Jul 2019.

S1. Experimental and Theoretical Methods

S1.1 Experimental

The chemicals and reagents, including nickel (II) chloride hexahydrate ($NiCl_2 \cdot 6H_2O$, 99.999%, Acros Organics), tetraoctyl-ammonium bromide (TOABr, $[CH_3(CH_2)_7]_4NBr$, 98%, Aldrich), sodium borohydride ($NaBH_4$, ≥98.0%, Sigma-

Aldrich), 2-phenylethanethiol (PET; $C_6H_5CH_2CH_2SH$, 98%, Sigma-Aldrich), H_2O_2 (30 %, Sigma-Aldrich), toluene (HPLC grade, Fisher Scientific), tetrahydrofuran (THF), dichloromethane (DCM) and methanol absolute (≥99.8%, Sigma-Aldrich) are commercially available and used as received.

The synthesis of $Ni_6(C_8H_9S)_{12}$ nanoclusters refers to the previously reported method.[1] Simply, $NiCl_2 \cdot 6H_2O$ (0.1000 g) and TOABr (0.488 g) were first dissolved in 100 mL of THF to give a deep-blue solution. The ligand 2-phenylethanethiol (0.290 mL) was added, and the reaction mixture was stirred for additional 5 minutes. This was followed by the addition of 14 mL solution of $NaBH_4$ (0.160 g) in deionized water. The formation of a dark-brown solution indicates successful formation of the nickel clusters. The reaction was kept stirring for 24 hours and the THF solvent was removed via rotary evaporation. The crude product was washed with methanol several times to remove the excess of redundant phenylethanethiol ligand. The isolated pure product was then crystallized by dissolving either in a minimum amount of CH_2Cl_2 or toluene with an equal volume of ethanol, and setting aside for slow evaporation of the solvents. Electrospray ionization mass spectrometry (ESI-MS), X-ray diffractometry (XRD), X-ray photoelectron spectroscopy (XPS) and Ultraviolet–Visible (UV-Vis) spectrometry were used for the characterization of the $Ni_6(C_8H_9S)_{12}$ cluster.

Toluene catalytic oxidation reactions were carried out in 50 mL round bottom flask under the conditions given in the Table 1. Gas chromatography-mass spectrometry (GC-MS) method was used for the analysis of the reaction products. Quantitative results

for the reactant conversion, product selectivity, and product yield were calculated by the following equations (1)–(3),

$$\text{Substrate conversion } \% = \frac{Moles\ of\ substrate\ reacted}{Inistial\ moles\ of\ substrate} \times 100 \quad (1)$$

$$\text{Product selectivity } \% = \frac{Moles\ of\ product\ formed}{Moles\ of\ substrate\ reacted} \times 100 \quad (2)$$

$$\text{Product yield } \% = \frac{Substrate\ conversion\ \%\ \times Product\ selectivity\ \%}{100} \quad (3)$$

S1.2 Theoretical Method

Density functional theory (DFT) calculations were conducted to investigate the thermodynamic process of toluene oxidation on Ni_6 clusters by using the Vienna ab initio Simulation Program (VASP) package.[2] The exchange and correlation potentials was described by PBE (Perdew, Burke, and Ernzerhof) functional generalized gradient approximation (GGA).[3] The nuclei-electron interactions were represented by the projector augmented wave (PAW) pseudopotentials.[4] van der Waals interactions were calculated by DFT-D3 method.[5] For the optimization of clusters and reaction intermediates, the kinetic energy cutoff of the plan wave basis was set to 400 eV with spin-polarizations. All atoms were allowed to relax until the electronic self-consistence and the ionic relaxation reaching the convergence criteria of 5×10^{-6} eV and 0.03 eV/Å. The reaction free energy of every elementary step was calculated as follows:

$$\Delta G = \Delta H - T\Delta S \quad (4)$$

Where ΔH presents the enthalpy changes given by electronic energy plus zero-point vibrations, and $T\Delta S$ corresponding to entropy changes. To simplify the calculation, the ligand of Ni_6 nanocluster was replaced by -SH group.

NBO analysis was performed using the related program implemented in the Gaussian 09,[6] with B3LYP functional,[3, 7] and 6-31G** basis set. The second order perturbative energy provides a measure of the overlap integral between the lone-pair orbital of the acceptor and the antibonding orbital of the donor. For each donor NBO (i) and acceptor NBO (j), the stabilization energy E(2) associated with delocalization is estimated as:

$$E(2) = \Delta E_{ij} = q_i \frac{F(i,j)^2}{\varepsilon_j - \varepsilon_i} \quad (5)$$

where q_i is the donor orbital occupancy, e_i, e_j are diagonal elements (orbital energies) and *F(i,j)* is the off-diagonal NBO Fock matrix element.

S2. Single crystal data

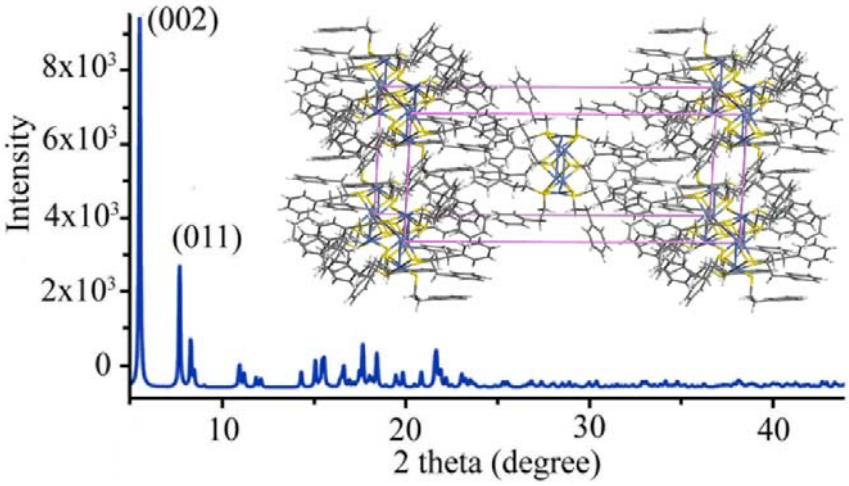

Figure S1. The XRD pattern of $Ni_6(C_8H_{10}S)_{12}$ cluster as obtained from single crystal X-ray analysis, with an inset showing the chemical structure.

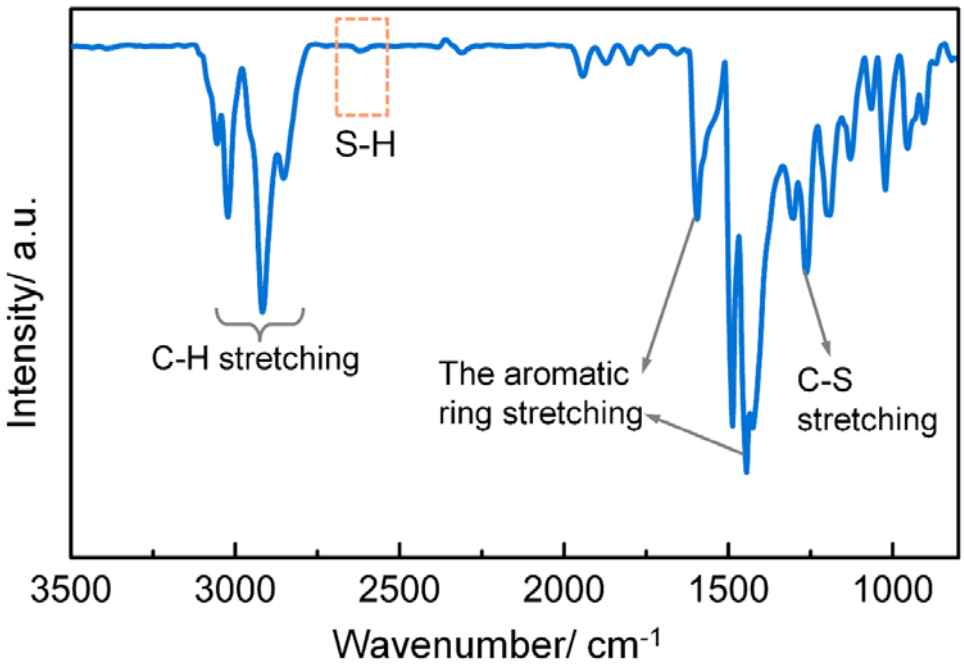

Figure S2. The IR pattern of as prepared $Ni_6(C_8H_{10}S)_{12}$ clusters, with the S-H bond being significantly weakened, comparing with the normal IR spectrum of the ligand (Nanoscale, 2014, 6, 9185)[8], indicative of the formation Ni-S bonds.

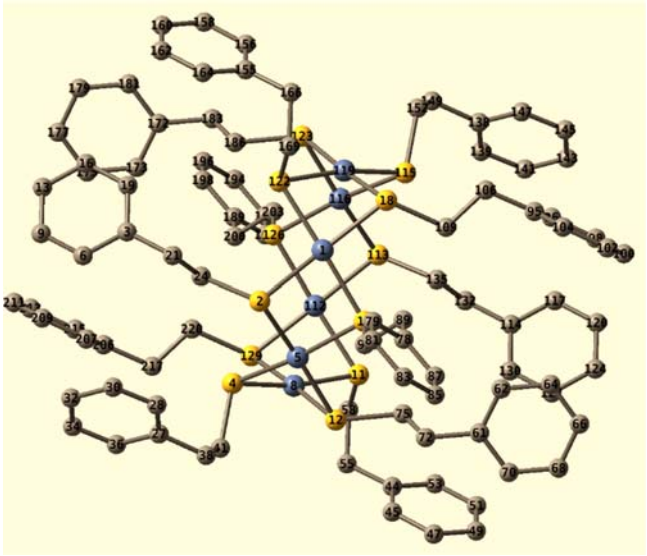

Figure S3. The structure and atomic numbering of the $Ni_6(C_8H_{10}S)_{12}$ cluster.

Table S1. The $Ni_6(C_8H_9S)_{12}$ single crystal data

Identification code	mx7095l	
Empirical formula	C96 H108 Ni6 S12	
Formula weight	1998.80	
Temperature	173.15 K	
Wavelength	0.71073 Å	
Crystal system	Monoclinic	
Space group	P 1 21/n 1	
Unit cell dimensions	a = 11.244(3) Å	α= 90°.
	b = 12.415(3) Å	β= 92.071(5)°.
	c = 32.461(9) Å	γ = 90°.
Volume	4528(2) $Å^3$	
Z	2	
Density (calculated)	1.466 Mg/m^3	
Absorption coefficient	1.545 mm^{-1}	
F(000)	2088	
Crystal size	0.171 x 0.142 x 0.051 mm^3	
Theta range for data collection	1.939 to 27.507°.	
Index ranges	-14<=h<=13, -16<=k<=15, -42<=l<=32	
Reflections collected	32180	
Independent reflections	10290 [R(int) = 0.0510]	
Completeness to theta = 25.242°	99.4 %	
Absorption correction	Semi-empirical from equivalents	
Max. and min. transmission	1.00000 and 0.85297	
Refinement method	Full-matrix least-squares on F^2	
Data / restraints / parameters	10290 / 0 / 514	
Goodness-of-fit on F^2	1.126	
Final R indices [I>2sigma(I)]	R1 = 0.0498, wR2 = 0.0836	
R indices (all data)	R1 = 0.0572, wR2 = 0.0872	
Extinction coefficient	n/a	
Largest diff. peak and hole	0.400 and -0.495 $e.Å^{-3}$	

Table S2. Bond lengths [Å] and angles [°] for mx7095l.

Ni1-S1	2.1937(9)
Ni1-Ni3#1	2.8382(9)
Ni1-S3#1	2.2026(9)
Ni1-S5	2.1920(9)
Ni1-S6	2.1903(9)
S1-Ni2	2.1968(9)
S1-C8	1.830(3)
C1-C2	1.391(4)
C1-C6	1.393(4)
C1-C7	1.515(4)
S2-Ni2	2.2108(10)
S2-Ni3	2.2252(9)
S2-C16	1.841(3)
Ni2-Ni3	2.9478(9)
Ni2-S4	2.2006(9)
Ni2-S5	2.1928(9)
C2-H2	0.9500
C2-C3	1.393(5)
Ni3-S3	2.2020(9)
Ni3-S4	2.1779(9)
Ni3-S6#1	2.1966(9)
C3-H3	0.9500
C3-C4	1.379(5)
S3-C24	1.836(3)
S4-C32	1.829(3)
C4-H4	0.9500
C4-C5	1.382(5)
S5-C40	1.845(3)
C5-H5	0.9500
C5-C6	1.391(4)
S6-C48	1.814(3)
C6-H6	0.9500
C7-H7A	0.9900
C7-H7B	0.9900
C7-C8	1.524(4)
C8-H8A	0.9900

C8-H8B	0.9900
C9-C10	1.391(4)
C9-C14	1.384(4)
C9-C15	1.511(4)
C10-H10	0.9500
C10-C11	1.388(5)
C11-H11	0.9500
C11-C12	1.381(5)
C12-H12	0.9500
C12-C13	1.385(5)
C13-H13	0.9500
C13-C14	1.390(5)
C14-H14	0.9500
C15-H15A	0.9900
C15-H15B	0.9900
C15-C16	1.525(4)
C16-H16A	0.9900
C16-H16B	0.9900
C17-C18	1.400(5)
C17-C22	1.382(5)
C17-C23	1.512(5)
C18-H18	0.9500
C18-C19	1.383(6)
C19-H19	0.9500
C19-C20	1.368(7)
C20-H20	0.9500
C20-C21	1.377(7)
C21-H21	0.9500
C21-C22	1.385(5)
C22-H22	0.9500
C23-H23A	0.9900
C23-H23B	0.9900
C23-C24	1.522(4)
C24-H24A	0.9900
C24-H24B	0.9900
C25-C26	1.394(4)
C25-C30	1.391(4)
C25-C31	1.517(4)

C26-H26	0.9500
C26-C27	1.387(4)
C27-H27	0.9500
C27-C28	1.385(5)
C28-H28	0.9500
C28-C29	1.383(5)
C29-H29	0.9500
C29-C30	1.386(5)
C30-H30	0.9500
C31-H31A	0.9900
C31-H31B	0.9900
C31-C32	1.524(4)
C32-H32A	0.9900
C32-H32B	0.9900
C33-C34	1.393(4)
C33-C38	1.392(4)
C33-C39	1.506(4)
C34-H34	0.9500
C34-C35	1.390(4)
C35-H35	0.9500
C35-C36	1.383(5)
C36-H36	0.9500
C36-C37	1.387(5)
C37-H37	0.9500
C37-C38	1.387(5)
C38-H38	0.9500
C39-H39A	0.9900
C39-H39B	0.9900
C39-C40	1.522(4)
C40-H40A	0.9900
C40-H40B	0.9900
C41-C42	1.400(4)
C41-C46	1.384(4)
C41-C47	1.517(4)
C42-H42	0.9500
C42-C43	1.376(5)
C43-H43	0.9500
C43-C44	1.385(5)

C44-H44	0.9500
C44-C45	1.387(5)
C45-H45	0.9500
C45-C46	1.387(4)
C46-H46	0.9500
C47-H47A	0.9900
C47-H47B	0.9900
C47-C48	1.532(4)
C48-H48A	0.9900
C48-H48B	0.9900

S1-Ni1-Ni3#1	132.58(3)
S1-Ni1-S3#1	98.55(4)
S3#1-Ni1-Ni3#1	49.87(2)
S5-Ni1-S1	82.54(3)
S5-Ni1-Ni3#1	118.27(3)
S5-Ni1-S3#1	163.69(3)
S6-Ni1-S1	176.56(3)
S6-Ni1-Ni3#1	49.78(2)
S6-Ni1-S3#1	81.51(3)
S6-Ni1-S5	98.38(3)
Ni1-S1-Ni2	86.55(3)
C8-S1-Ni1	113.41(10)
C8-S1-Ni2	112.79(10)
C2-C1-C6	118.1(3)
C2-C1-C7	120.0(3)
C6-C1-C7	121.9(3)
Ni2-S2-Ni3	83.29(3)
C16-S2-Ni2	103.48(11)
C16-S2-Ni3	107.60(10)
S1-Ni2-S2	99.00(4)
S1-Ni2-Ni3	138.63(3)
S1-Ni2-S4	171.68(3)
S2-Ni2-Ni3	48.56(3)
S4-Ni2-S2	82.46(3)
S4-Ni2-Ni3	47.36(2)
S5-Ni2-S1	82.45(3)
S5-Ni2-S2	170.57(3)

S5-Ni2-Ni3	125.35(3)
S5-Ni2-S4	97.46(3)
C1-C2-H2	119.5
C1-C2-C3	121.0(3)
C3-C2-H2	119.5
Ni1#1-Ni3-Ni2	115.328(16)
S2-Ni3-Ni1#1	122.41(3)
S2-Ni3-Ni2	48.15(2)
S3-Ni3-Ni1#1	49.89(2)
S3-Ni3-S2	167.82(3)
S3-Ni3-Ni2	123.29(3)
S4-Ni3-Ni1#1	130.74(3)
S4-Ni3-S2	82.64(3)
S4-Ni3-Ni2	48.01(2)
S4-Ni3-S3	96.50(3)
S4-Ni3-S6#1	176.46(3)
S6#1-Ni3-Ni1#1	49.59(2)
S6#1-Ni3-S2	100.03(3)
S6#1-Ni3-Ni2	135.53(3)
S6#1-Ni3-S3	81.38(3)
C2-C3-H3	120.0
C4-C3-C2	119.9(3)
C4-C3-H3	120.0
Ni3-S3-Ni1#1	80.24(3)
C24-S3-Ni1#1	109.45(10)
C24-S3-Ni3	106.87(11)
Ni3-S4-Ni2	84.63(3)
C32-S4-Ni2	112.87(10)
C32-S4-Ni3	114.79(10)
C3-C4-H4	120.0
C3-C4-C5	119.9(3)
C5-C4-H4	120.0
Ni1-S5-Ni2	86.69(3)
C40-S5-Ni1	112.24(10)
C40-S5-Ni2	104.77(10)
C4-C5-H5	120.0
C4-C5-C6	120.0(3)
C6-C5-H5	120.0

Ni1-S6-Ni3#1	80.63(3)
C48-S6-Ni1	115.88(10)
C48-S6-Ni3#1	113.25(10)
C1-C6-H6	119.5
C5-C6-C1	121.0(3)
C5-C6-H6	119.5
C1-C7-H7A	108.7
C1-C7-H7B	108.7
C1-C7-C8	114.1(2)
H7A-C7-H7B	107.6
C8-C7-H7A	108.7
C8-C7-H7B	108.7
S1-C8-H8A	109.4
S1-C8-H8B	109.4
C7-C8-S1	111.0(2)
C7-C8-H8A	109.4
C7-C8-H8B	109.4
H8A-C8-H8B	108.0
C10-C9-C15	119.1(3)
C14-C9-C10	118.2(3)
C14-C9-C15	122.6(3)
C9-C10-H10	119.4
C11-C10-C9	121.2(3)
C11-C10-H10	119.4
C10-C11-H11	120.0
C12-C11-C10	120.0(3)
C12-C11-H11	120.0
C11-C12-H12	120.4
C11-C12-C13	119.2(3)
C13-C12-H12	120.4
C12-C13-H13	119.7
C12-C13-C14	120.5(3)
C14-C13-H13	119.7
C9-C14-C13	120.7(3)
C9-C14-H14	119.6
C13-C14-H14	119.6
C9-C15-H15A	107.8
C9-C15-H15B	107.8

C9-C15-C16	118.0(3)
H15A-C15-H15B	107.2
C16-C15-H15A	107.8
C16-C15-H15B	107.8
S2-C16-H16A	109.0
S2-C16-H16B	109.0
C15-C16-S2	113.0(2)
C15-C16-H16A	109.0
C15-C16-H16B	109.0
H16A-C16-H16B	107.8
C18-C17-C23	120.5(3)
C22-C17-C18	118.2(3)
C22-C17-C23	121.3(3)
C17-C18-H18	119.9
C19-C18-C17	120.2(4)
C19-C18-H18	119.9
C18-C19-H19	119.8
C20-C19-C18	120.5(4)
C20-C19-H19	119.8
C19-C20-H20	119.8
C19-C20-C21	120.4(4)
C21-C20-H20	119.8
C20-C21-H21	120.3
C20-C21-C22	119.4(4)
C22-C21-H21	120.3
C17-C22-C21	121.4(4)
C17-C22-H22	119.3
C21-C22-H22	119.3
C17-C23-H23A	108.8
C17-C23-H23B	108.8
C17-C23-C24	113.7(3)
H23A-C23-H23B	107.7
C24-C23-H23A	108.8
C24-C23-H23B	108.8
S3-C24-H24A	109.3
S3-C24-H24B	109.3
C23-C24-S3	111.6(2)
C23-C24-H24A	109.3

C23-C24-H24B	109.3
H24A-C24-H24B	108.0
C26-C25-C31	121.5(3)
C30-C25-C26	118.4(3)
C30-C25-C31	120.0(3)
C25-C26-H26	119.4
C27-C26-C25	121.1(3)
C27-C26-H26	119.4
C26-C27-H27	120.1
C28-C27-C26	119.8(3)
C28-C27-H27	120.1
C27-C28-H28	120.2
C29-C28-C27	119.6(3)
C29-C28-H28	120.2
C28-C29-H29	119.7
C28-C29-C30	120.6(3)
C30-C29-H29	119.7
C25-C30-H30	119.8
C29-C30-C25	120.4(3)
C29-C30-H30	119.8
C25-C31-H31A	108.6
C25-C31-H31B	108.6
C25-C31-C32	114.8(2)
H31A-C31-H31B	107.6
C32-C31-H31A	108.6
C32-C31-H31B	108.6
S4-C32-H32A	109.9
S4-C32-H32B	109.9
C31-C32-S4	108.9(2)
C31-C32-H32A	109.9
C31-C32-H32B	109.9
H32A-C32-H32B	108.3
C34-C33-C39	121.4(3)
C38-C33-C34	117.9(3)
C38-C33-C39	120.6(3)
C33-C34-H34	119.4
C35-C34-C33	121.1(3)
C35-C34-H34	119.4

C34-C35-H35	120.1
C36-C35-C34	119.9(3)
C36-C35-H35	120.1
C35-C36-H36	120.0
C35-C36-C37	120.0(3)
C37-C36-H36	120.0
C36-C37-H37	120.2
C38-C37-C36	119.6(3)
C38-C37-H37	120.2
C33-C38-H38	119.3
C37-C38-C33	121.5(3)
C37-C38-H38	119.3
C33-C39-H39A	109.0
C33-C39-H39B	109.0
C33-C39-C40	113.1(2)
H39A-C39-H39B	107.8
C40-C39-H39A	109.0
C40-C39-H39B	109.0
S5-C40-H40A	109.8
S5-C40-H40B	109.8
C39-C40-S5	109.2(2)
C39-C40-H40A	109.8
C39-C40-H40B	109.8
H40A-C40-H40B	108.3
C42-C41-C47	120.5(3)
C46-C41-C42	118.4(3)
C46-C41-C47	121.1(3)
C41-C42-H42	119.6
C43-C42-C41	120.7(3)
C43-C42-H42	119.6
C42-C43-H43	119.9
C42-C43-C44	120.2(3)
C44-C43-H43	119.9
C43-C44-H44	120.0
C43-C44-C45	119.9(3)
C45-C44-H44	120.0
C44-C45-H45	120.2
C44-C45-C46	119.6(3)

C46-C45-H45	120.2
C41-C46-C45	121.2(3)
C41-C46-H46	119.4
C45-C46-H46	119.4
C41-C47-H47A	109.1
C41-C47-H47B	109.1
C41-C47-C48	112.3(2)
H47A-C47-H47B	107.9
C48-C47-H47A	109.1
C48-C47-H47B	109.1
S6-C48-H48A	109.9
S6-C48-H48B	109.9
C47-C48-S6	109.1(2)
C47-C48-H48A	109.9
C47-C48-H48B	109.9
H48A-C48-H48B	108.3

Symmetry transformations used to generate equivalent atoms:

#1 -x+1,-y+1,-z+1

S3. GC-MS analysis

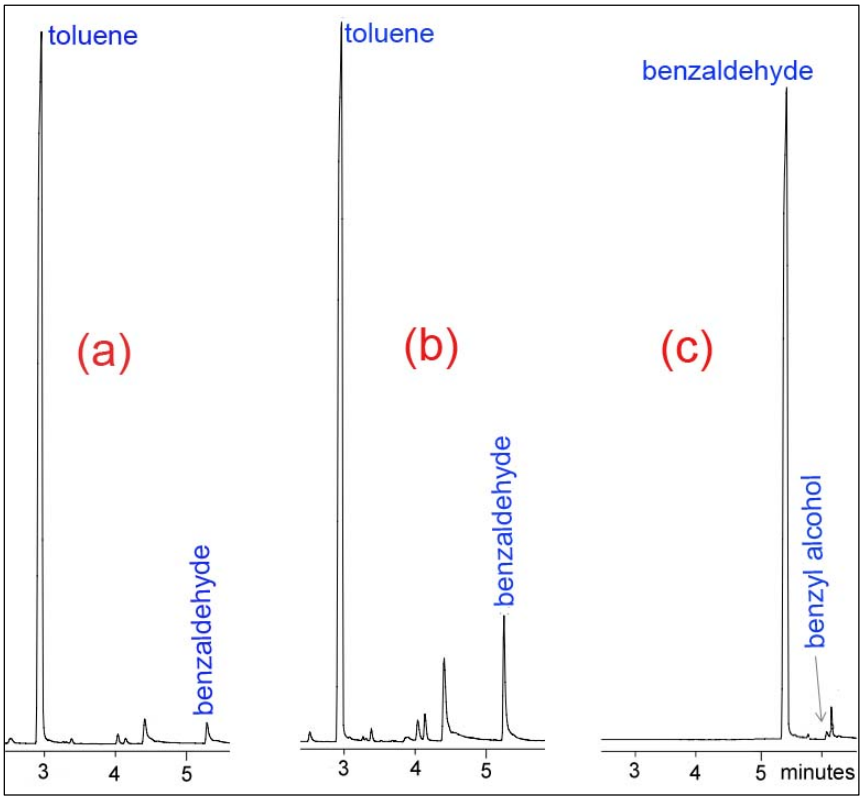

Figure S4. Product profile obtained from oxidation of toluene in terms of GC response time; (a) 1 hour (b) 2 hours (c) 4 hours in the presence of H_2O_2 at 80 ^oC. A conversion of 100% is indicated in the case of (c).

S4. DFT calculation details

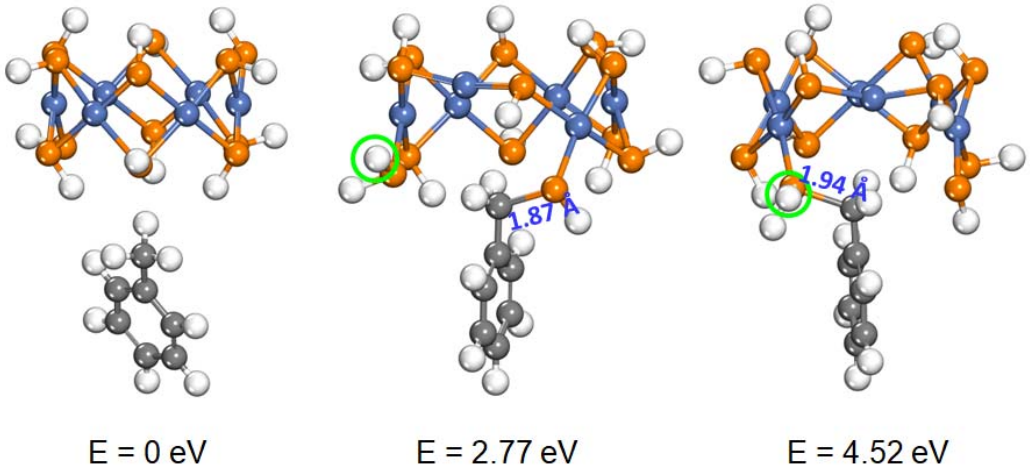

Figure S5. The initial structure and two final structures of toluene directly react with Ni_6 clusters. The corresponding energies are shown below each configuration. The hydrogen atom marked in circle is represented the dissociated hydrogen from toluene.

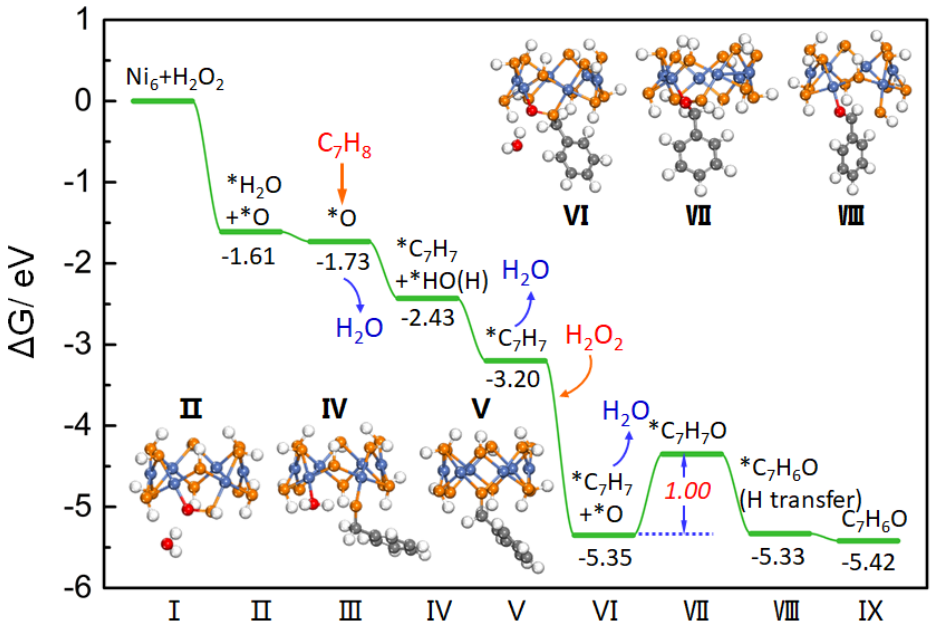

Figure S6. Another possible reaction pathway for oxidation of toluene to benzaldehyde.

Table S3. Second order perturbation theory analysis of Fock matrix in NBO donor–acceptor interactions in naked Ni_6 without any ligands.

Donor	Acceptor	E(2), eV
211. BD*(1)Ni 1 -Ni 2	/ 76. LP (4)Ni 2	0.1895
215. BD*(1)Ni 4 -Ni 5	/ 94. LP (4)Ni 5	0.1895
213. BD*(1)Ni 2 -Ni 3	/ 76. LP (4)Ni 2	0.1882
216. BD*(1)Ni 5 -Ni 6	/ 94. LP (4)Ni 5	0.1882
211. BD*(1)Ni 1 -Ni 2	/ 70. LP (4)Ni 1	0.1444
215. BD*(1)Ni 4 -Ni 5	/ 85. LP*(4)Ni 4	0.1444
213. BD*(1)Ni 2 -Ni 3	/ 82. LP*(4)Ni 3	0.1422
216. BD*(1)Ni 5 -Ni 6	/ 97. LP*(4)Ni 6	0.1422
212. BD*(1)Ni 1 -Ni 6	/ 70. LP (4)Ni 1	0.1179
214. BD*(1)Ni 3 -Ni 4	/ 85. LP*(4)Ni 4	0.1179
212. BD*(1)Ni 1 -Ni 6	/ 97. LP*(4)Ni 6	0.1171
214. BD*(1)Ni 3 -Ni 4	/ 82. LP*(4)Ni 3	0.1171
24. CR (3)Ni 2	/ 72. LP*(6)Ni 1	0.0941
51. CR (3)Ni 5	/ 87. LP*(6)Ni 4	0.0941
24. CR (3)Ni 2	/ 84. LP*(6)Ni 3	0.0932
51. CR (3)Ni 5	/ 99. LP*(6)Ni 6	0.0932
2. BD (1)Ni 1 -Ni 3	/ 77. LP*(5)Ni 2	0.0806
11. BD (1)Ni 4 -Ni 6	/ 95. LP*(5)Ni 5	0.0806
33. CR (3)Ni 3	/121. RY*(1)Ni 2	0.0720
60. CR (3)Ni 6	/175. RY*(1)Ni 5	0.0720
15. CR (3)Ni 1	/121. RY*(1)Ni 2	0.0715
42. CR (3)Ni 4	/175. RY*(1)Ni 5	0.0715
1. BD (1)Ni 1 -Ni 2	/213. BD*(1)Ni 2 -Ni 3	0.0659
9. BD (1)Ni 4 -Ni 5	/216. BD*(1)Ni 5 -Ni 6	0.0659
5. BD (1)Ni 2 -Ni 3	/211. BD*(1)Ni 1 -Ni 2	0.0655
12. BD (1)Ni 5 -Ni 6	/215. BD*(1)Ni 4 -Ni 5	0.0655
70. LP (4)Ni 1	/ 72. LP*(6)Ni 1	0.0629
15. CR (3)Ni 1	/ 99. LP*(6)Ni 6	0.0598
42. CR (3)Ni 4	/ 84. LP*(6)Ni 3	0.0598
1. BD (1)Ni 1 -Ni 2	/212. BD*(1)Ni 1 -Ni 6	0.0572
9. BD (1)Ni 4 -Ni 5	/214. BD*(1)Ni 3 -Ni 4	0.0572
5. BD (1)Ni 2 -Ni 3	/214. BD*(1)Ni 3 -Ni 4	0.0568
12. BD (1)Ni 5 -Ni 6	/212. BD*(1)Ni 1 -Ni 6	0.0568
33. CR (3)Ni 3	/ 87. LP*(6)Ni 4	0.0564
60. CR (3)Ni 6	/ 72. LP*(6)Ni 1	0.0564
4. BD (1)Ni 1 -Ni 6	/211. BD*(1)Ni 1 -Ni 2	0.0525
8. BD (1)Ni 3 -Ni 4	/215. BD*(1)Ni 4 -Ni 5	0.0525
4. BD (1)Ni 1 -Ni 6	/216. BD*(1)Ni 5 -Ni 6	0.0520
8. BD (1)Ni 3 -Ni 4	/213. BD*(1)Ni 2 -Ni 3	0.0520
76. LP (4)Ni 2	/121. RY*(1)Ni 2	0.0494
94. LP (4)Ni 5	/175. RY*(1)Ni 5	0.0494
76. LP (4)Ni 2	/ 70. LP (4)Ni 1	0.0455
94. LP (4)Ni 5	/ 85. LP*(4)Ni 4	0.0455

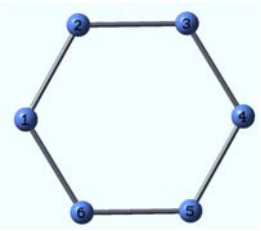

Table S4. Second order perturbation theory analysis of Fock matrix in NBO donor–acceptor interactions in naked Ni_6 without any ligands.

Donor	Acceptor	E(2),eV
492. LP*(6)Ni 8	/484. LP*(7)Ni 5	4.96
537. LP*(6)Ni 119	/529. LP*(7)Ni 116	4.96
483. LP*(6)Ni 5	/493. LP*(7)Ni 8	4.35
528. LP*(6)Ni 116	/538. LP*(7)Ni 119	4.35
537. LP*(6)Ni 119	/469. LP*(7)Ni 1	4.00
492. LP*(6)Ni 8	/514. LP*(7)Ni 112	4.00
468. LP*(6)Ni 1	/538. LP*(7)Ni 119	3.76
513. LP*(6)Ni 112	/493. LP*(7)Ni 8	3.76
468. LP*(6)Ni 1	/484. LP*(7)Ni 5	2.38
513. LP*(6)Ni 112	/529. LP*(7)Ni 116	2.38
484. LP*(7)Ni 5	/469. LP*(7)Ni 1	1.78
529. LP*(7)Ni 116	/514. LP*(7)Ni 112	1.78
528. LP*(6)Ni 116	/514. LP*(7)Ni 112	1.69
483. LP*(6)Ni 5	/469. LP*(7)Ni 1	1.69
495. LP*(9)Ni 8	/513. LP*(6)Ni 112	1.20
540. LP*(9)Ni 119	/468. LP*(6)Ni 1	1.20
498. LP (3) S 11	/492. LP*(6)Ni 8	0.83
543. LP (3) S 122	/537. LP*(6)Ni 119	0.83
507. LP (3) S 18	/537. LP*(6)Ni 119	0.81
552. LP (3) S 129	/492. LP*(6)Ni 8	0.81
495. LP*(9)Ni 8	/483. LP*(6)Ni 5	0.80
540. LP*(9)Ni 119	/528. LP*(6)Ni 116	0.80
501. LP (3) S 12	/483. LP*(6)Ni 5	0.78
546. LP (3) S 123	/528. LP*(6)Ni 116	0.78
477. LP (3) S 4	/483. LP*(6)Ni 5	0.78
522. LP (3) S 115	/528. LP*(6)Ni 116	0.78
501. LP (3) S 12	/492. LP*(6)Ni 8	0.77
546. LP (3) S 123	/537. LP*(6)Ni 119	0.77
507. LP (3) S 18	/468. LP*(6)Ni 1	0.76
552. LP (3) S 129	/513. LP*(6)Ni 112	0.76
477. LP (3) S 4	/492. LP*(6)Ni 8	0.75
522. LP (3) S 115	/537. LP*(6)Ni 119	0.75
474. LP (3) S 2	/484. LP*(7)Ni 5	0.72
519. LP (3) S 113	/529. LP*(7)Ni 116	0.72
477. LP (3) S 4	/493. LP*(7)Ni 8	0.71
522. LP (3) S 115	/538. LP*(7)Ni 119	0.71
501. LP (3) S 12	/493. LP*(7)Ni 8	0.70
546. LP (3) S 123	/538. LP*(7)Ni 119	0.70
543. LP (3) S 122	/468. LP*(6)Ni 1	0.69
474. LP (3) S 2	/469. LP*(7)Ni 1	0.69
498. LP (3) S 11	/513. LP*(6)Ni 112	0.69
519. LP (3) S 113	/514. LP*(7)Ni 112	0.69
474. LP (3) S 2	/468. LP*(6)Ni 1	0.68
519. LP (3) S 113	/513. LP*(6)Ni 112	0.68
507. LP (3) S 18	/538. LP*(7)Ni 119	0.67
552. LP (3) S 129	/493. LP*(7)Ni 8	0.67
538. LP*(7)Ni 119	/469. LP*(7)Ni 1	0.67
493. LP*(7)Ni 8	/514. LP*(7)Ni 112	0.67
504. LP (3) S 15	/468. LP*(6)Ni 1	0.66
549. LP (3) S 126	/513. LP*(6)Ni 112	0.66
498. LP (3) S 11	/493. LP*(7)Ni 8	0.64
543. LP (3) S 122	/538. LP*(7)Ni 119	0.64
498. LP (3) S 11	/514. LP*(7)Ni 112	0.64
543. LP (3) S 122	/469. LP*(7)Ni 1	0.64
504. LP (3) S 15	/484. LP*(7)Ni 5	0.63
549. LP (3) S 126	/529. LP*(7)Ni 116	0.63
504. LP (3) S 15	/469. LP*(7)Ni 1	0.63
549. LP (3) S 126	/514. LP*(7)Ni 112	0.63
507. LP (3) S 18	/469. LP*(7)Ni 1	0.62
552. LP (3) S 129	/514. LP*(7)Ni 112	0.62
501. LP (3) S 12	/484. LP*(7)Ni 5	0.62
546. LP (3) S 123	/529. LP*(7)Ni 116	0.62

477. LP (3) S 4	/484. LP*(7)Ni 5	0.59
522. LP (3) S 115	/529. LP*(7)Ni 116	0.59
504. LP (3) S 15	/483. LP*(6)Ni 5	0.58
549. LP (3) S 126	/528. LP*(6)Ni 116	0.58
473. LP (2) S 2	/483. LP*(6)Ni 5	0.58
518. LP (2) S 113	/528. LP*(6)Ni 116	0.58
474. LP (3) S 2	/483. LP*(6)Ni 5	0.55
519. LP (3) S 113	/528. LP*(6)Ni 116	0.55
475. LP (1) S 4	/485. LP*(8)Ni 5	0.50
520. LP (1) S 115	/530. LP*(8)Ni 116	0.50
502. LP (1) S 15	/485. LP*(8)Ni 5	0.50
547. LP (1) S 126	/530. LP*(8)Ni 116	0.50
505. LP (1) S 18	/538. LP*(7)Ni 119	0.50
550. LP (1) S 129	/493. LP*(7)Ni 8	0.50
472. LP (1) S 2	/484. LP*(7)Ni 5	0.49
517. LP (1) S 113	/529. LP*(7)Ni 116	0.49
496. LP (1) S 11	/515. LP*(8)Ni 112	0.48
541. LP (1) S 122	/470. LP*(8)Ni 1	0.48
496. LP (1) S 11	/494. LP*(8)Ni 8	0.48
541. LP (1) S 122	/539. LP*(8)Ni 119	0.48
472. LP (1) S 2	/469. LP*(7)Ni 1	0.47
517. LP (1) S 113	/514. LP*(7)Ni 112	0.47
475. LP (1) S 4	/494. LP*(8)Ni 8	0.47
520. LP (1) S 115	/539. LP*(8)Ni 119	0.47
492. LP*(6)Ni 8	**/529. LP*(7)Ni 116**	**0.47**

References

1. Kagalwala, H. N.; Gottlieb, E.; Li, G.; Li, T.; Jin, R.; Bernhard, S., Photocatalytic hydrogen generation system using a nickel-thiolate hexameric cluster. *Inorg. Chem.* **2013,** *52* (15), 9094-9101.
2. Kresse, G.; Furthmüller, J., Efficient iterative schemes for ab initio total-energy calculations using a plane-wave basis set. *Phys. Rev. B* **1996,** *54* (16), 11169-11186.
3. Perdew, J. P.; Burke, K.; Ernzerhof, M., Generalized gradient approximation made simple. *Phys. Rev. Lett.* **1996,** *77* (4), 3865-3868.
4. Kresse, G.; Joubert, D., From ultrasoft pseudopotentials to the projector augmented-wave method. *Phys. Rev. B* **1999,** *59* (3), 1758-1775.
5. Grimme, S.; Antony, J.; Ehrlich, S.; Krieg, H., A consistent and accurate ab initio parametrization of density functional dispersion correction (DFT-D) for the 94 elements H-Pu. *J. Chem. Phys.* **2010,** *132* (15).
6. Glendening, E.; Reed, A.; Carpenter, J.; Weinhold, F., NBO Version 3.1, TCI. *University of Wisconsin, Madison* **1998,** *65*.
7. Dunning Jr, T. H., Gaussian basis sets for use in correlated molecular calculations. I. The atoms boron through neon and hydrogen. *J. Chem. Phys.* **1989,** *90* (2), 1007-1023.
8. Ji, J.; Wang, G.; Wang, T.; You, X.; Xu, X., Thiolate-protected Ni 39 and Ni 41 nanoclusters: synthesis, self-assembly and magnetic properties. *Nanoscale* **2014,** *6* (15), 9185-9191.

1. Kagalwala, H. N.; Gottlieb, E.; Li, G.; Li, T.; Jin, R.; Bernhard, S., Photocatalytic hydrogen generation system using a nickel-thiolate hexameric cluster. *Inorg. Chem.* **2013,** *52* (15), 9094-9101.
2. Kresse, G.; Furthmüller, J., Efficient iterative schemes for ab initio total-energy calculations using a plane-wave basis set. *Phys. Rev. B* **1996,** *54* (16), 11169-11186.
3. Perdew, J. P.; Burke, K.; Ernzerhof, M., Generalized gradient approximation made simple. *Phys. Rev. Lett.* **1996,** *77* (4), 3865-3868.
4. Kresse, G.; Joubert, D., From ultrasoft pseudopotentials to the projector augmented-wave method. *Phys. Rev. B* **1999,** *59* (3), 1758-1775.

5. Grimme, S.; Antony, J.; Ehrlich, S.; Krieg, H., A consistent and accurate ab initio parametrization of density functional dispersion correction (DFT-D) for the 94 elements H-Pu. *J. Chem. Phys.* **2010,** *132* (15).
6. Glendening, E.; Reed, A.; Carpenter, J.; Weinhold, F., NBO Version 3.1, TCI. *University of Wisconsin, Madison* **1998,** *65*.
7. Dunning Jr, T. H., Gaussian basis sets for use in correlated molecular calculations. I. The atoms boron through neon and hydrogen. *J. Chem. Phys.* **1989,** *90* (2), 1007-1023.